Journal of the European Ceramic Society 21 (2001) 1425–1428

www.elsevier.com/locate/jeurceramsoc

Crack initiation and crack propagation in partially electroded PZT

S.L. dos Santos e Lucato *, D.C. Lupascu, J. Rödel

Institute of Materials Science, Darmstadt University of Technology, Petersenstr. 23, D-64287 Darmstadt, Germany

Received 4 September 2000; accepted 13 November 2000

Abstract

For partially electroded piezoelectric materials, a strain incompatibility arises between the electrically active part and the electrically inactive part of the material. This can lead to crack initiation and crack propagation perpendicular to the electrode edge. In order to study crack initiation, a symmetrical geometry with the electrodes in the centre of the surfaces of thin lead zirconate titanate (PZT) plates was devised. Upon application of the electrical field, different cracking patterns appear, depending on degree of coverage and on thickness of the plates. Linear and non-linear FEM modelling is able to explain some of the materials response.

Keywords: Actuators; Defects; Fracture; PZT

1. Introduction

Ceramic actuators have been accepted for numerous applications such as low frequency high amplitude devices in adaptive structures and vibration control.[1,2] Applications range from aircraft and automobiles to printing and textile machinery. In actuator applications, ferroelectrics frequently fracture under high electric fields or mechanical stresses. The limited reliability of the component due to cracking constitutes a major impediment to large scale usage.

The most cost efficient geometry for such actuators has the disadvantage of electrodes ending inside the ceramic. A strain incompatibility due to inactive regions next to active material in the actuator is the consequence. High mechanical stresses at these areas lead to crack formation and finally to the failure of the device. Several investigations were made in the past to understand the underlying mechanisms.[3–5] Cracks due to thermal strain mismatch have been studied in other materials such as metal/ceramics[6] and ceramics.[7]

In this work initiation and propagation of cracks formed by strain incompatibility during the first poling cycle in partially electroded PZT specimens are investigated. A geometry representing a single layer of a multilayer device was chosen (Fig. 1). The focus is laid on the geometrical influence to crack formation and the initial crack growth. To rationalise some of the mechanisms linear and non-linear finite element modelling was done.

The strain mismatch was achieved by using small rectangular specimens with centred electrodes as shown in Fig. 1. If an electric field is applied to the specimen the material between the electrodes will shrink in directions perpendicular to the field and expand in direction of the applied electrical field. As the adjacent material is not affected by the electric field it will mechanically clamp the active strip and high stresses arise.

2. Experimental procedure

2.1. Specimen preparation

All experiments were performed on a commercially available lead zirconate titanate, namely PZT 151 (PI Ceramics, Lederhose, Germany). The samples were delivered as plates of dimensions 40×40 mm^2 with thicknesses of 1 and 2 mm and were polished on one side to a 1 μm finish. Some of the 1 mm thick plates were ground down to 0.5 mm after polishing. Finally the plates were cut to specimens with approx. 10×10 mm^2.

In the next step electrodes of Au / Pd were sputtered on the specimens. To achieve only partial coverage masks of overhead foil were cut and attached to both surfaces with superglue and removed after sputtering.

* Corresponding author. Tel.: +49-6151-16-6312; fax: +49-6151-16-6314.

E-mail address: lucato@ceramics.tu-darmstadt.de (S.L. dos Santos e Lucato).

0955-2219/01/$ - see front matter
PII: S0955-2219(01)00033-4

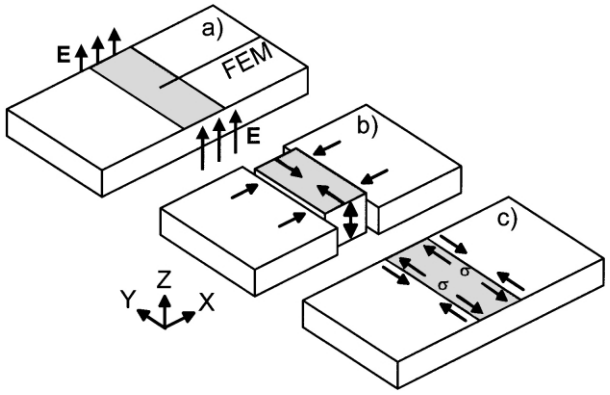

Fig. 1. Illustration of stresses generated by mechanical clamping due to partial electrode coverage. (a) Electric field is applied on the centred electrodes (active material). (b) Shrinkage in X and Y directions and expansion in Z direction of the active part. (c) Adjacent material mechanically clamps the active strip and high stresses arise. The area modelled with the non-linear FEM code is shown in (a).

The electrodes had a final thickness of approx. 50 nm. A thin line of silver-paint was applied on both electrodes to ensure complete contact of the electrodes in case of cracking. As a last step thin copper wires were mounted on the electrodes with a conducting 2-component epoxy-glue. Ten different geometries were prepared, being thicknesses of 0.5 mm, 1 mm and 2 mm each with electrode widths of 1, 2 and 4 mm plus a fully electroded specimen with a thickness of 2 mm.

A co-ordinate system for further orientation was set up as follows. Direction Z is the electrical field direction. Y is parallel to the electrode edge and X is perpendicular thereto. The electrode coverage is defined by $2b/2w$, were $2b$ is the electrode width and 2w the specimen width. The volume between the electrodes will be defined as active material and the remainder inactive material.

2.2. Mapping of the crack-patterns

A half electrical cycle (0–2 kV/mm at 25 V/mm s) has been applied to specimens of all nine partially covered geometries. The crack-patterns were then mapped in an optical microscope at a magnification of 200×. To do so, the wires were removed from the plates and the silver–paint was carefully washed off with acetone. The specimens were then placed on a co-ordinate desk attached to the microscope and the crack tips were targeted with the crosshairs in the eye pieces. A computer determined the co-ordinates and transferred them to a custom designed CAD-type software.

2.3. Crack growth measurement

The crack growth measurement was done in-situ in an optical microscope at 200× magnification. A small open plastic box mounted on the co-ordinate desk filled with Flourinert® was used for specimen fixture and electrical insulation. The electrical field was increased in small steps up to 3.5 kV/mm and the length of the first crack on each electrode edge was measured after each step. A geometry of approx. $10\times10\times1$ mm^3 with an electrode width of 1 mm was chosen for this test.

2.4. Finite element modelling

Two finite element modelling approaches were made. In the first approach the experiment was modelled three-dimensionally using the linear piezoelectric element (Solid 5) of a commercial FEM-Code (Ansys® 5.5). The electrodes were implemented by coupling the voltage degree of freedom of the surface nodes. As the electrodes on the real specimens were very thin it was not necessary to model the electrode material. The piezoelectric and mechanical coefficients provided by the manufacturer have been used. For symmetry reasons only a quarter of the specimen was modelled.

To visualise the electric fields, the resulting dielectric displacement and the mechanical stresses a custom designed non-linear FEM-code[8] was used. The material data was as of a 8/65/35 PLZT. As the modelled material shows qualitatively the same behaviour as the investigated PZT no effort was made to adapt the code to the data of our material. The upper half of a two-dimensional slice perpendicular to the electrode edge was modelled as shown in Fig. 1a.

3. Results

Two types of cracks have to be distinguished. Fig. 2 (left) shows the resulting crack patterns for three geometries. For wide electrodes only short cracks at the electrode edges formed. The narrower electrodes contain long cracks that extend from one side to the other and separate the electrode in two and more fractions. Long cracks were only found in some specimens with narrow electrodes up to 20% coverage and do always appear in electrodes with a coverage of 10%. They are usually formed from two small cracks that join.

The number of short cracks formed mainly depends on the specimen thickness whereas the length of the starter cracks are dependent on the electrode coverage. Numerous cracks are found in the 2 mm thick specimens and only few in the 0.5 mm specimens. The lengths of the largest short cracks ranged from approx. 200 to 400 μm in the narrow electrodes and up to approx. 600–900 μm in the wide electrodes. Variations of the crack-lengths could not be correlated to the specimen thickness.

The short starter cracks are developed at an electrical field somewhat lower than the coercive field of 1 kV/mm (Fig. 3b). They all appear within a very small field range. By further increasing the field some grow faster than others and those slower cracks are closed as the

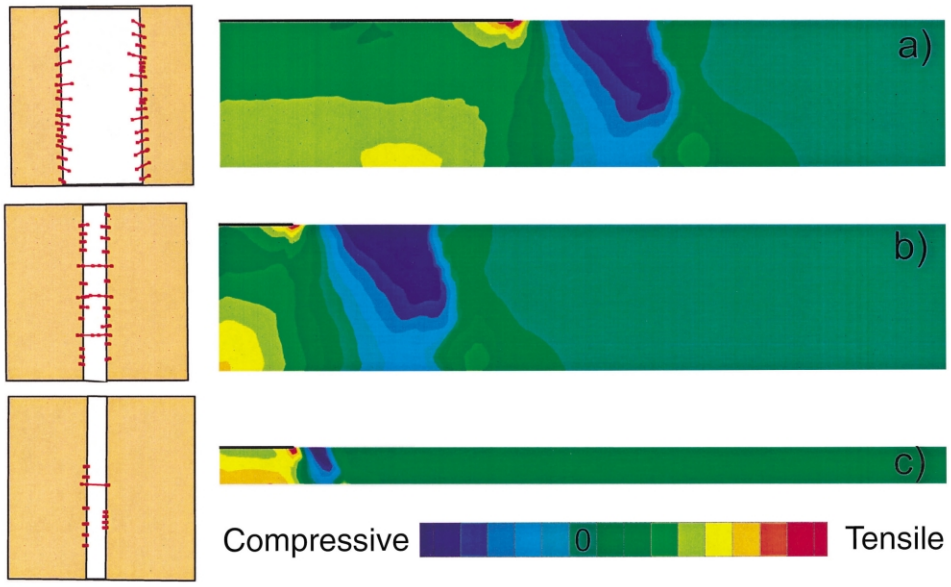

Fig. 2. Observed crack-patterns and calculated stresses perpendicular to the electrode. Specimen dimensions are of (a) 2/4, (b) 2/1 and (c) 0.5/1 (thickness (mm)/electrode width (mm)].

stress is relieved by the faster cracks. A decrease in the number of visible cracks is the result. The region between 0.9 and 1.25 kV/mm is characterised by the fastest crack growth (Fig. 3a). Above 1.25 kV/mm the cracks grow approximately linear with the electric field and finally at about 3.5 kV/mm the specimen saturates and the crack growth is stopped. This behaviour agrees very well with the strain hysteresis[9] obtained for that material.

In the case of narrow electrodes some of the starter cracks joined and formed large cracks. Fig. 3a shows the crack lengths of two opposing small cracks. The filled dots represent the inner part of the cracks. It can be seen that the inner and the outer part of the cracks initially grow with the same rate. At 1.05 kV/mm the inner parts have attained a critical length and join by unstable growth.

On specimens with 4 mm electrode the cracks do not grow perpendicular to the electrode edge as it would be expected, but a radial crack growth is observed (Fig. 2a left). Only cracks at the centre of the specimen do show the expected direction. That effect is not seen in 1 mm electrodes and only to a smaller extent on 2 mm electrodes. The crack growth direction is reproduced regardless of the specimen thickness and is only determined by the electrode coverage.

4. Discussion

Crack formation at the electrode edges and the variation of the number of cracks for different thicknesses can be explained by processes at the electrode edges. There,

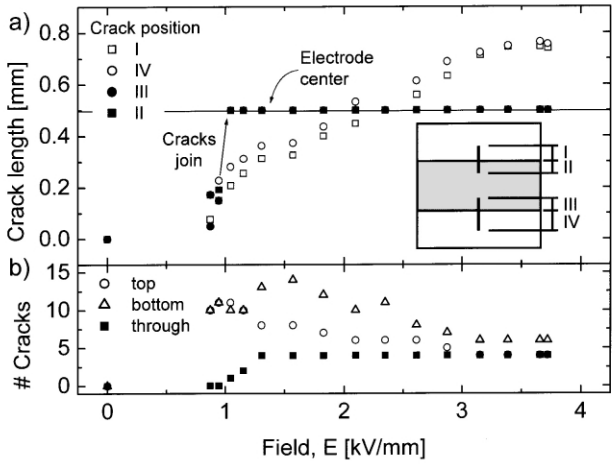

Fig. 3. (a) Crack lengths measured from the originating electrode edge. The inner cracks join at 1.05 kV/mm. (b) Amount of cracks on both electrode edges and amount of joined cracks.

an electrical field singularity within the material is generated[10] and, due to the electromechanical coupling, gives rise to a mechanical stress singularity. The effect is enhanced by the fact that the specimens were unpoled at the beginning. Domains near the electrode edges will experience a higher electrical field due to the singularity and will switch earlier than the neighbouring domains. Consequently, a very high strain incompatibility and accompanying stresses between the switched volume and the bulk are obtained, in particular at fields near the coercive field of the bulk ceramic. Crack initiation at the electrode edges at a global electric field below the coercive field results. The mechanical stresses as calculated

by non-linear FEM parallel to the electrode edges (Y-direction) are shown in Fig. 2 (right). A zone of high tensile stresses is located directly underneath the electrode edge. Outside of the electrodes an area of compressive stresses with a width of about half the thickness is apparent. Far outside the specimen is stress-free. In the centre of the active material the tensile stresses increase from the top to the centre of the specimen.

The size of the zone where high stresses are obtained is greatly increased in the thick specimens as compared to the thin specimens. This is a further manifestation of electromechanical coupling since the volume with a certain electrical field within the singularity depends on the applied voltage. The voltage, however, has to be increased in thicker specimens to obtain the same electric field in the bulk. As failure in ceramics is governed by weakest link statistics, both the magnitude of local stresses as well as their extension are crucial. Therefore, more cracks are formed in thick specimens since the volume of high stresses around the electrode edge is larger.

Mechanical edge effects are equally responsible for the deviation of the crack growth direction from a direction perpendicular to the electrode edges. The first principal stresses on the specimen surface as calculated by a linear piezoelectric FEM are shown in Fig. 4. The actual crack pattern obtained for a specimen of the modelled geometry is overlaid. It can clearly be seen that the cracks grow perpendicular to the first principal stresses. Due to piezoelectric deformations of the specimen shear stresses

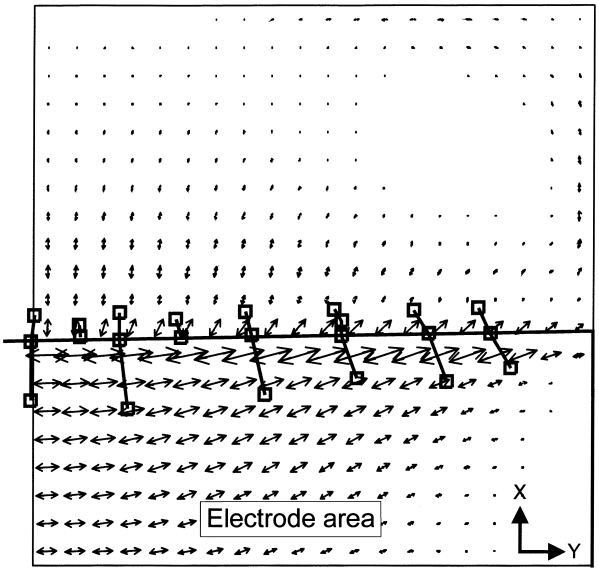

Fig. 4. Top view on the direction and magnitude of the first principal stresses in a quarter of the specimen. The crack pattern obtained from a real specimen is overlaid.

are introduced in a large volume of the specimen. In fact, only a very small region around the X centre line is not affected. A comparison to specimen with less electrode coverage shows that the shear stresses influenced a zone approximately equal to the electrode width.

5. Conclusions

(a) The electric field singularity at the electrode edge leads to a zone of very high tensile stresses responsible for formation of cracks during the first poling.

(b) The number of electrode edge cracks increases with increasing thickness as the stressed volume grows.

(c) Long cracks can occur as the result of coalescence of two short electrode edge cracks.

(d) The direction of the short cracks is governed by mechanical edge effects caused by shear stresses.

Acknowledgements

The authors greatly acknowledge the support of this work by the Deutsche Forschungsgemeinschaft (DFG) under contract No. Rö 954/13.

References

1. Uchino, K., *Piezoelectric Actuators and Ultrasonic Motors*. Kluwer Academic, Boston, 1997.
2. Haertling, G. H., Ferroelectric ceramics. History and technology. *J. Am. Ceram. Soc.*, 1999, **82**(4), 797–818.
3. Schneider, G. A., Rostek, A., Zickgraf, B. and Aldinger, F., Crack growth in ferroelectric ceramics under mechanical and electrical loading. In *Electroceramics IV*, ed. R. Waser, S. Bonnenberg, D. Bonnenberg and C. Hoffmann. Augustinus Buchhandlung, Aachen, 1994, pp. 1211–1216.
4. Schneider, G. A., Weitzing, H. and Zickgraf, B., Crack growth in ferroelectric ceramics and actuators under mechanical and electrical loading. *Frac. Mech. Ceram.*, 1996, **12**, 149–160.
5. Furuta, A. and Uchino, K., Dynamic observation of crack propagation in piezoelectric multilayer actuators. *J. Am. Ceram. Soc.*, 1993, **76**(6), 1615–1617.
6. Bartlett, A., Evans, A. G. and Rühle, M., Residual stress of metal/ceramic bonds. *Acta Metall. Mater*, 1991, **39**(7), 1579–1585.
7. Evans, A. G., Thermal fracture in ceramic materials. *Proc. Br. Ceram. Soc.*, 1975, **21**, 217–237.
8. Chen, W. and Lynch, C. S., Finite element analysis of cracks in ferroelectric ceramic materials. *Eng. Fract. Mech.*, 1999, **64**, 539–562.
9. dos Santos e Lucato, S. L., Lupascu, D. C. and Rödel, J., Effect of poling direction on R-curve behavior in lead zirconate titanate. *J. Am. Ceram. Soc.*, 2000, **83**(2), 424–426.
10. Gong, X. Y. and Suo, Z., Reliability of ceramic multilayer actuators: a nonlinear finite element simulation. *J. Mech. Phys. Solids*, 1996, **44**(5), 751–769.